SIAM J. Applied Dynamical Systems
Vol. 8, No. 3, pp. 1324–1340

Splay States in a Ring of Coupled Oscillators: From Local to Global Coupling*

Wei Zou† and Meng Zhan‡

Abstract. In this work, we study dynamical behavior in a ring of coupled nonlinear oscillators and focus on the stability of homogeneous steady state and splay states by performing linear stability analysis. Different cases from local (nearest-neighbor) coupling to global (all-to-all) coupling by increasing the range of coupling are studied. Some explicit stability results for each possible splay state are analytically obtained. It is valuable to compare their similarities and differences for these different cases. All these results could shed improved light on our understanding of the organization of splay states in coupled oscillators.

Key words. coupled nonlinear oscillators, splay state, steady state, local coupling, global coupling, linear stability

AMS subject classifications. 34C15, 37G15, 37G35, 65L07

DOI. 10.1137/09075398X

1. Introduction.

Collective behavior in coupled nonlinear oscillators has attracted great interest among researchers in nonlinear science due to its significance for both dynamics theory and various applications [1, 2, 3, 4]. One of the important collective behaviors, splay state, in which all oscillators take an identical periodic orbit but with a (constant) phase difference between them, has been extensively studied [5, 6, 7, 8, 9, 10, 11, 12, 13, 14, 15, 16, 17, 18, 19, 20, 21, 22, 23, 24, 25, 26]. It appears to be a very general phenomenon, and it has been observed in such diverse systems as Josephson-junction arrays [6, 7, 8, 9, 10, 11, 12], electronic oscillator circuits [13], arrays of laser models [15, 16, 17, 18, 19], coupled phase models [20, 21], and biological systems [22, 23], to name only a few. Clearly it can play important roles in the pattern (or structure) formations and self-organizations in coupled systems. In the literature, the term "splay state" was also called "antiphase (or splay-phase) state" [5], "ponies on a merry-go-round" [12], "periodic traveling (or rotating) wave" [13, 14], "waltz state" [16], etc.

In most of existing works, splay state has been studied in globally coupled systems, and some unusual properties have been reported so far, including (1) attractor crowding [6, 7], in which the number of system attractors increases dramatically with the increase of the oscillator number and, consequently, the volume occupied by each attractor gets extremely small and the coupled systems become extremely sensitive to noise, and (2) the neutral stability of splay

*Received by the editors March 26, 2009; accepted for publication (in revised form) by B. Ermentrout July 30, 2009; published electronically September 23, 2009. This work was partially supported by the Outstanding Oversea Scholar Foundation of Chinese Academy of Sciences (Bairenjihua), the National Natural Science Foundation of China under grant 10675161, and a grant from The Scientific Research Foundation for the Returned Overseas Chinese Scholars, State Education Ministry.
http://www.siam.org/journals/siads/8-3/75398.html
†Graduate School of the Chinese Academy of Sciences, Beijing 100049, China (zouwei05@mails.gucas.ac.cn).
‡Corresponding author. Wuhan Institute of Physics and Mathematics, Chinese Academy of Sciences, Wuhan 430071, China (zhanmeng@wipm.ac.cn).

states with more than one zero eigenvalues existing in a large parameter space [8, 9, 10, 11, 12], in contrast to our common sense that any neutral stability of state can occur only at special parameter points, when a state is at the crossover from stable to unstable (or vice versa). Comparatively, splay state in locally coupled systems has been less studied [18, 24, 25, 26], to the best knowledge of the authors. For recent developments, some researchers [27, 28] found that splay state may even appear in chaotic systems, if the concept of splay state is redefined and the average distribution of phase of chaotic oscillators is considered. In [29, 30], Zhan and authors uncovered a novel generalized splay state in extremely weakly coupled chaotic oscillators, in which all chaotic oscillators transit to a periodic state with an identical periodic orbit and taking different and functionally related phases. Very recently, Zhan and Kapral [31, 32] generalized the concept of splay state to an Archimedean spiral splay field, in which a spiral wave in a two-dimensional space is considered to be a special splay state where spatial points having identical phase space orbits take phases determined by the Archimedean spiral on which they lie. Again, the splay state can be periodic or chaotic. On the basis of this simplification, the spatial structure of line defects in complex oscillatory spiral waves [31] and the destruction of chaotic spiral waves [32] have been well analyzed.

The purpose of this work is to investigate dynamical behaviors in a ring of coupled nonlinear oscillators. Both the homogeneous steady state and splay states for each wave number will be treated. Based on rigorous mathematical analyses of linear stability of these states, explicit stability results are obtained. As a special case of splay states for a zero wave number, the stability of an in-phase state can also be easily analyzed. In our model study, we conveniently set a system parameter to characterize the range of coupling of systems, and thus by tuning it we are able to study coupled systems under different situations, from local coupling to global coupling via intermediate-range coupling. Results show that different coupling ranges change the system dynamics tremendously.

The remainder of this paper is organized as follows. In section 2, we give our model and solutions of the model including the homogeneous steady state and splay states. We will analyze their respective stabilities in sections 3 and 4, the main parts of the paper. Finally, section 5 is devoted to some brief discussions. Some useful matrices and their relations are given in Appendix A. The detailed analysis on the stability of the general splay state is presented in Appendix B.

2. Model and solutions. Consider a popular model of N coupled Landau–Stuart oscillators,

$$\dot{z_j} = (a + i\omega - |z_j|^2)z_j + \varepsilon \sum_{m=1}^{d} (z_{j+m} + z_{j-m} - 2z_j), \qquad j = 1, \ldots, N, \tag{1}$$

where a is a parameter specifying the distance from Hopf bifurcation, ω is the natural frequency, both of which are set to be identical for each oscillator, ε is the coupling strength, and d denotes the coupling range. Periodic boundary conditions are considered, namely, $z_{j+N} = z_j$ for all j. This ring configuration is a simple description for some coupled systems in nature and is easy for analysis. Both positive and negative coupling ε (corresponding to the usual

phase-attractive and phase-repulsive coupling, respectively) will be investigated. For different coupling ranges d, two extreme cases exist: One is the local (nearest-neighbor, diffusive-type) coupling for $d = 1$, and the other is the global (all-to-all, mean-field) coupling for $d = \frac{N-1}{2}$ (N being odd). It is interesting to change d and study the system dynamics.

For a single Landau–Stuart oscillator in the absence of coupling, the dynamics is well known [2]: If $a < 0$, a steady state staying at the origin is stable, whereas if $a > 0$, this steady state loses stability and the system generates a new stable limit cycle, whose rotation semidiameter is $\sqrt{a}$ and rotation frequency is ω. This bifurcation is a supercritical Hopf bifurcation, and the parameter a at $a = 0$ is usually called the Hopf bifurcation point. As the Landau–Stuart oscillator model is the normal form of Hopf bifurcation, the model of coupled Landau–Stuart oscillators has been extensively studied, and some intriguing dynamical behaviors have been reported so far, e.g., amplitude death [33, 34, 35], ultraharmonic oscillations (or multifrequency oscillations) [36, 37], intermittent switching [38], diffusion-induced inhomogeneity [39], aging transition [40, 41, 42], and destabilization patterns [43]. Obviously this model study is of significance for both experimental observations and theoretical development.

The homogeneous steady state for all oscillators staying at the origin,

$$|z_1| = |z_2| = \cdots = |z_N| = r = 0, \tag{2}$$

is a solution to (1), which has been termed *off state* in [18].

Except for this solution, the splay state solutions can also be easily obtained,

$$\begin{aligned} &|z_1| = |z_2| = \cdots = |z_N| = r_k = \sqrt{a + \varepsilon\sigma_k}, \\ &\theta_j = \omega t + \frac{2k\pi}{N}(j-1), \\ &j = 1, \ldots, N, \quad k = 0, \ldots, N-1, \end{aligned} \tag{3}$$

where

$$\sigma_k = -4 \sum_{m=1}^{d} \sin^2\left(\frac{mk\pi}{N}\right) \leq 0, \tag{4}$$

under the assumption that all oscillators have the same size semidiameter and the only difference is the phase difference $\frac{2k\pi}{N}$ between any neighboring oscillators. They exist based on an obvious existence condition,

$$a + \varepsilon\sigma_k \geq 0. \tag{5}$$

Physically, k denotes the wave number of systems and each k represents different modes of splay states. A special case is $k = 0$, representing the in-phase, synchronous state, whose stability can be easily obtained as a special case in the analysis of splay states, as we will see below. Due to the geometric symmetry of the coupled systems, the splay states of k and $N - k$ are equivalent. Therefore, in the following analysis, we need only to consider the modes $k = 0, 1, \ldots, [\frac{N}{2}]$, with $[\xi]$ denoting the greatest integer number less than or equal to ξ.

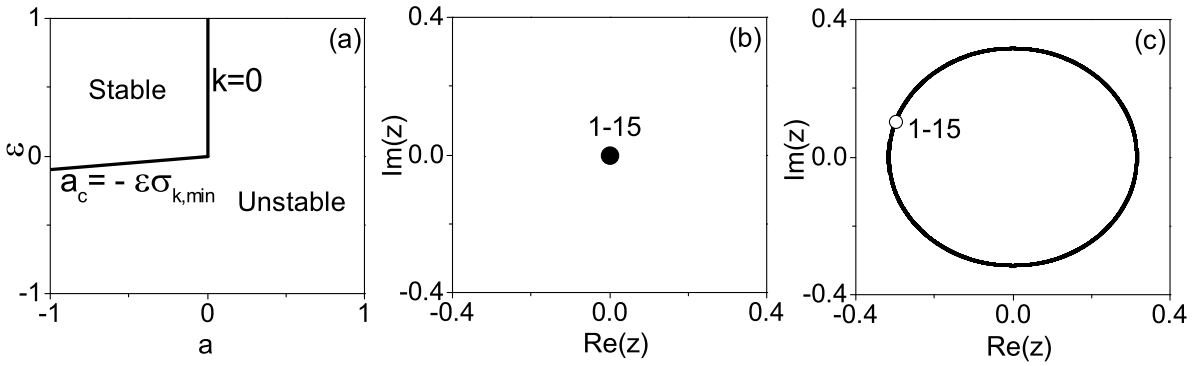

Figure 1. (a) *The stable and unstable regions of the homogeneous steady state. The stable region is surrounded by two critical curves (one a vertical curve, $a = 0$ ($\varepsilon > 0$), and the other a sloped curve, $a_c = -\varepsilon\sigma_{k,min}$ ($\varepsilon < 0$)).* (b) *and* (c) *The attractors and snapshots of oscillators at one time instant of the homogeneous steady state ($a = -0.5$ and $\varepsilon = 0.5$) and the in-phase state ($a = 0.1$ and $\varepsilon = 0.2$) born due to the instability of the homogeneous steady state, respectively. $d = 2$ and $N = 15$.*

3. Stability analysis of the homogeneous steady state. In this section, we will analyze the stability of the homogeneous steady state (equation (2)). With respect to the solution, the linearization equation is

$$\dot{y_j} = (a + i\omega)y_j + \varepsilon \sum_{m=1}^{d} (y_{j+m} + y_{j-m} - 2y_j), \qquad j = 1, \ldots, N. \tag{6}$$

Its eigenvalues can be calculated as

$$\lambda_k = a + \varepsilon\sigma_k \pm i\omega, \quad k = 0, 1, \ldots, N-1. \tag{7}$$

If $\mathrm{Re}(\lambda_k) = a + \varepsilon\sigma_k < 0$ for all k, the state is stable; otherwise, it is unstable. From (7), we have $\lambda_k = \lambda_{N-k}$. Thus, we may consider only $k = 0, 1, \ldots, [\frac{N}{2}]$.

Under the condition of $\varepsilon > 0$, if $a < 0$, then $\mathrm{Re}(\lambda_k) < 0$ definitely as $\sigma_k \leq 0$. However, if a becomes positive, $\mathrm{Re}(\lambda_0) = a$ for $k = 0$ becomes positive (with $\mathrm{Re}(\lambda_k)$ staying negative for all other k's). As a result, the homogeneous steady state loses stability at $a = 0$ and $\varepsilon > 0$ and the systems may generate a splay state of the $k = 0$ mode (the in-phase state) at the same time. This situation is similar to that of a single Landau–Stuart oscillator. Therefore, $a = 0$ ($\varepsilon > 0$) is a Hopf bifurcation curve of coupled systems. With a increasing further, larger k modes may get unstable step by step. As shown in Figure 1(a), on the left side of the vertical line in the (a, ε) parameter plane, the homogeneous steady state is stable, and oppositely on the right, the in-phase state ($k = 0$) is stable. As one example, we plot the attractors of all oscillators within and outside of the stable regime in Figures 1(b) and 1(c) for the parameters ($a = -0.5$ and $\varepsilon = 0.5$) and ($a = 0.1$ and $\varepsilon = 0.2$), respectively, which clearly show the corresponding dynamical behaviors as the theoretical analysis. In numerical simulations, we have chosen $\omega = 2.0$ and $N = 15$, which are fixed throughout the paper. Clearly, this stable-unstable division line at $a = 0$ and $\varepsilon > 0$ for the homogeneous steady state and the in-phase state does not change with different d's.

However, if $\varepsilon < 0$, one immediate condition for the stability of the homogeneous steady state is $a < 0$, as $\sigma_k \leq 0$. In particular, the stable-unstable division line a_c should be determined by the first unstable mode, namely,

$$a_c = -\varepsilon \sigma_{k,min}, \tag{8}$$

where $\sigma_{k,min}$ denotes the minimum value among σ_k $(k = 0, \ldots, [\frac{N}{2}])$ and k_{min} represents the corresponding k. Now $a = 0$ is no longer the Hopf bifurcation point of the systems and the phase-repulsive coupling ($\varepsilon < 0$) effectively reduces the Hopf bifurcation threshold, as shown with the sloped curve in Figure 1(a); this bifurcation has been called coupling-induced Hopf bifurcation in [26]. More detailed information about $\sigma_{k,min}$ for different d can be analyzed.

(a) If $d = 1$ for the local coupling,

$$\sigma_{k,min} = -4 \sin^2 \left(\frac{k\pi}{N} \right). \tag{9}$$

Consequently, we have

$$\sigma_{k,min} = \begin{cases} -4 & \text{for } k_{min} = \frac{N}{2} \text{ (even } N\text{)}, \\ -4 \sin^2(\frac{N-1}{2N}\pi) & \text{for } k_{min} = \frac{N-1}{2} \text{ (odd } N\text{)}. \end{cases} \tag{10}$$

The value of k_{min} is exactly the middle one among all k's.

(b) Oppositely, if $d = \frac{N-1}{2}$ and N is odd for the global coupling, we have

$$\sigma_{k,min} = -4 \sum_{m=1}^{\frac{N-1}{2}} \sin^2 \left(\frac{mk\pi}{N} \right) = -N, \tag{11}$$

as

$$\sum_{m=1}^{N} \sin^2 mx = \frac{2N+1}{4} - \frac{\sin(2N+1)x}{4 \sin x}.$$

It is notable that $\sigma_{k,min}$ does not depend on k $(k \neq 0)$.

(c) Unlike the above two extreme cases, for the intermediate coupling range, we cannot obtain k_{min} and $\sigma_{k,min}$ explicitly, and we have to rely on numerical simulations. In Figures 2(a)–2(d), we plot the distributions of σ_k on k for different coupling ranges: $d = 1$ (local coupling), 7 (global coupling), 2 (short intermediate coupling), and 4 (long intermediate coupling), respectively. Their corresponding splay states with the parameters chosen out of the stable regime and near the sloped curve in Figure 1(a) are illustrated in Figures 2(e)–2(h), respectively. These dynamical behaviors exactly indicate the corresponding k_{min} obtained from the analyses of σ_k (top row). For instance, $k_{min} = 4$ and 2 from Figures 2(c) and 2(d), respectively. In Figure 2(f), for the case of the global coupling due to the simultaneous changes of stability of all modes, a more scattered distribution of oscillators from random initial conditions, which has been termed general splay state by some researchers [19], is displayed. Clearly the general splay state ($\theta_j = \omega t + \varphi_j$ and $\sum_{j=1}^{N} e^{i\varphi_j} = 0$) exists in a more general manner. For some special set of initial conditions, a regularly distributed splay state for each mode can be locally stable and observable. For random initial conditions, however, the general splay state, such as in Figure 2(f), can be more easily found instead, because the basin of general splay is expected to be much larger than that of the regularly distributed splay state.

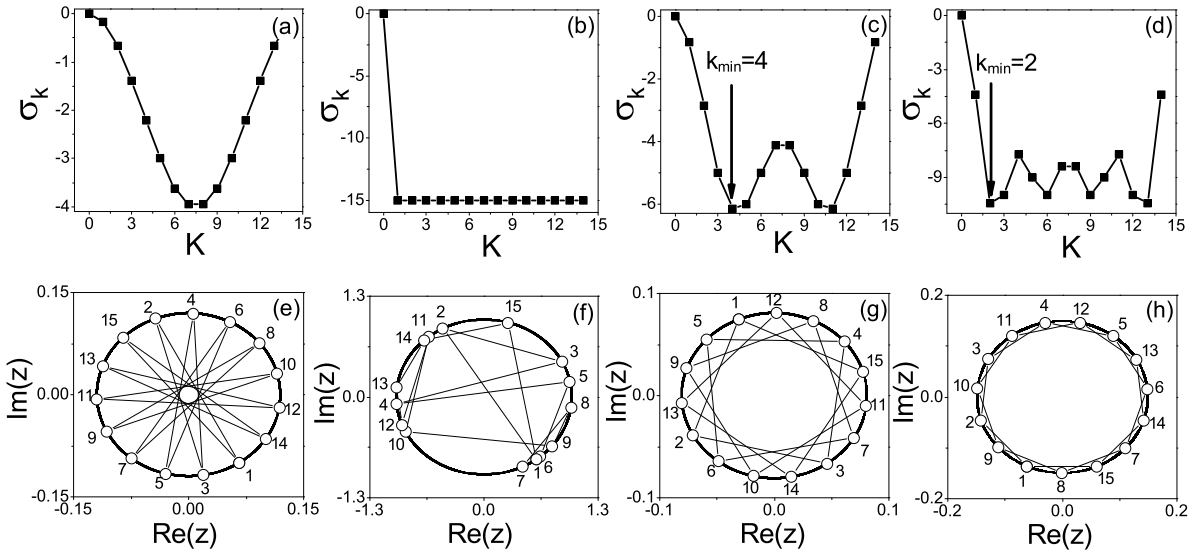

Figure 2. (a)–(d) *The dependence of σ_k (equation (4)) on k for $d = 1$, 7, 2, and 4, respectively.* (e)–(h) *The corresponding splay states with k_{min} obtained from the top row for the parameters $(a = -0.5, \varepsilon = -0.13)$, $(a = -0.5, \varepsilon = -0.1)$, $(a = -0.61, \varepsilon = -0.1)$, and $(a = -0.5, \varepsilon = -0.05)$, respectively. These parameters are chosen out of the stable regime and near the sloped curve in Figure 1(a). All instant positions of oscillators are indicated by open circles.*

4. Stability analysis of the splay states.

4.1. Common conditions. Similar to the analysis in the above section, the linearization equation with respect to the solution of splay states (equation (3)) is

$$\dot{y_j} = (a - 2r_k^2 + i\omega)y_j - r_k^2 e^{i2\theta_j}\overline{y_j} + \varepsilon \sum_{m=1}^{d}(y_{j+m} + y_{j-m} - 2y_j), \qquad j = 1, \ldots, N, \tag{12}$$

with $\overline{A}$ representing the conjugate of A (A is an arbitrary matrix). Setting $Y = (y_1, \ldots, y_N)'$, where the prime denotes the transposition of matrix or vector, we can write the equation in a compact form,

$$\dot{Y} = (a - 2r_k^2 + i\omega)Y - r_k^2 e^{i2\omega t} P_k^2 \overline{Y} + \varepsilon BY. \tag{13}$$

Refer to the matrices B and P_k in Appendix A, where B denotes the circular matrix and P_k denotes the diagonal matrix. Letting $Y = P_k PX$ (referring to the matrices P, S, and Λ_k in Appendix A), we can transform it into

$$\dot{X} = (a - 2r_k^2 + i\omega)X - r_k^2 e^{i2\omega t} S\overline{X} + \varepsilon \Lambda_k X, \tag{14}$$

and letting $X = \Delta Z e^{i\omega t}$ in order to eliminate the time-dependent term in (14), we further have

$$\dot{\Delta Z} = (a - 2r_k^2)\Delta Z - r_k^2 S\overline{\Delta Z} + \varepsilon \Lambda_k \Delta Z \tag{15}$$

and

$$\dot{\overline{\Delta Z}} = (a - 2r_k^2)\overline{\Delta Z} - r_k^2 S\Delta Z + \varepsilon\Lambda_k\overline{\Delta Z}. \tag{16}$$

They can be rewritten in a compact form as

$$\begin{pmatrix} \dot{\Delta Z} \\ \dot{\overline{\Delta Z}} \end{pmatrix} = M \begin{pmatrix} \Delta Z \\ \overline{\Delta Z} \end{pmatrix}, \tag{17}$$

with

$$M = \begin{pmatrix} M_1 & M_2 \\ M_2 & M_1 \end{pmatrix} \tag{18}$$

and the submatrices

$$M_1 = (a - 2r_k^2)I_N + \varepsilon\Lambda_k, \quad M_2 = -r_k^2 S. \tag{19}$$

As M is a real symmetric matrix, all of its eigenvalues are real. We have

$$|M| = |M_1 + M_2||M_1 - M_2|, \tag{20}$$

where $|A|$ denotes the determinant of A (A is an arbitrary matrix). It is easy to show explicitly that the eigenvalues of the matrix M are the same as those of the matrices $M_1 \pm M_2$, whose eigenvalues can be obtained from the following characteristic equations:

$$\lambda^2 - \alpha_j\lambda + \beta_j = 0, \quad j = 0, \ldots, \left[\frac{N}{2}\right], \tag{21}$$

with

$$\alpha_j = 2(a - 2r_k^2) + \varepsilon(\sigma_{k+j} + \sigma_{k-j}), \tag{22}$$

$$\beta_j = (a - 2r_k^2 + \varepsilon\sigma_{k+j})(a - 2r_k^2 + \varepsilon\sigma_{k-j}) - r_k^4. \tag{23}$$

For the number of eigenvalues, if N is odd, the eigenvalue equation for $j = 0$ has two eigenvalues, and that for the other values has four eigenvalues (considering the same form of equations for j and $N-j$.) Thus, the total number of eigenvalues is $2+\frac{N-1}{2}\times 4 = 2N$. In contrast, if N is even, the equations for both $j = 0$ and $j = \frac{N}{2}$ have two eigenvalues and the equation for the other values has four. Thus, the total number is unchanged: $2+2+(\frac{N}{2}-1)\times 4 = 2N$.

For some special cases, we may have simple forms of eigenvalues. For example, if $j = 0$, we have two eigenvalues: 0 and $-2r_k^2$ ($-2r_k^2 < 0$). Clearly the first zero eigenvalue and the second negative eigenvalue are necessary for the periodic solution of splay states for any k. If $k = 0$, we have the eigenvalues $\varepsilon\sigma_j$ and $\varepsilon\sigma_j - 2r_k^2$ for $j = 0, 1, \ldots, [\frac{N}{2}]$. After considering the stability condition ($\varepsilon\sigma_j < 0$) and the existence condition in (5), we conclude that this in-phase splay state is stable if $\varepsilon > 0$ and $a > 0$; namely, its stable regime is located in the upper-right corner of the (a, ε) parameter space from $\theta = 0$ to $\theta = \frac{\pi}{2}$, which obviously does not change

with d. This point is very important, and it can be viewed as one of the common features of coupled systems.

Next let us analyze the stability condition for any nonzero k. From (21), the sufficient and necessary conditions for the stable splay state of mode k are

$$\alpha_j \le 0 \quad \text{and} \quad \beta_j \ge 0, \quad j = 1, \dots, \left[\frac{N}{2}\right]. \tag{24}$$

With $\alpha_{j,max}$ ($\beta_{j,min}$) being the maximum (minimum) value among α_j (β_j), we need

$$\alpha_{j,max} \le 0 \tag{25}$$

and

$$\beta_{j,min} \ge 0. \tag{26}$$

We will refer to these inequalities as α and β (stability) conditions, respectively. In what follows, we will go further from these conditions (including the existence and stability conditions) for the three different cases: local coupling, global coupling, and intermediate-range coupling, separately.

4.2. Local coupling. In this subsection, we will discuss the case of local coupling for $d = 1$. Now $\sigma_k = -4\sin^2(\frac{k\pi}{N})$, and the existence condition (5) becomes

$$a \ge 4\varepsilon \sin^2\left(\frac{k\pi}{N}\right). \tag{27}$$

If $j = [\frac{N}{2}] = \frac{N}{2}$ for even N, a pair of eigenvalues of stability equation (21) are $-4\varepsilon\cos(\frac{2k\pi}{N})$ and $-4\varepsilon\cos(\frac{2k\pi}{N}) - 2r_k^2$. Obviously for any stable splay state of k mode, we need

$$\varepsilon \cos\left(\frac{2k\pi}{N}\right) \ge 0; \tag{28}$$

namely, the modes $0 \le k < \frac{N}{4}$ might be stable for $\varepsilon > 0$, and the modes $\frac{N}{4} < k \le \frac{N}{2}$ might be stable for $\varepsilon < 0$. This finding is the same as the observation in [24], where, however, further mathematical analyses for each mode in detail were unavailable. This restriction is also right for odd N; we have carefully checked this condition for small N numerically, and the above analysis is the same for odd N if N is large.

As $d = 1$, we have

$$\sigma_{k+j} + \sigma_{k-j} = -8\left(\sin^2\frac{k\pi}{N} + \cos\frac{2k\pi}{N}\sin^2\frac{j\pi}{N}\right), \tag{29}$$

$$\sigma_{k+j}\sigma_{k-j} = 16\left(\sin^2\frac{k\pi}{N} - \sin^2\frac{j\pi}{N}\right)^2. \tag{30}$$

Using inequality (28), we obtain

$$\alpha_{j,max} = \alpha_0 = -2r_k^2 \le 0. \tag{31}$$

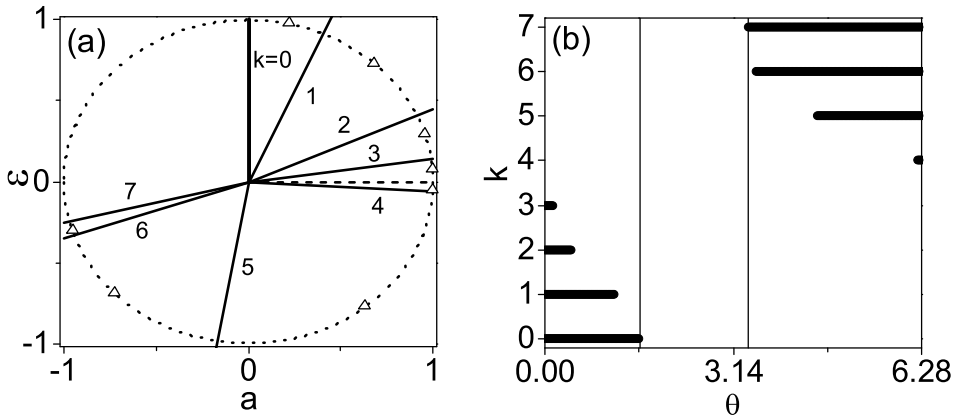

Figure 3. *The study of the local coupling ($d = 1$).* (a) *Schematic show of the stability distribution of all splay states for different k's based on the β condition (except the $k = 0$ mode). They are surrounded by their corresponding critical curve and the horizontal (dashed) curve ($\varepsilon = 0$, $a > 0$).* (b) *Numerical results for the dependence of the stable splay state regions for each k on the polar angle θ. The blank region surrounded by the two vertical lines represents the stable region of the homogeneous steady state. In numerics, random initial conditions very close to each splay state were chosen.*

Obviously, now the α condition is always fulfilled if this solution exists.

For the β condition,

$$\beta_j = 16\varepsilon^2 \sin^4 \frac{j\pi}{N} - \left(32\varepsilon^2 \sin^2 \frac{k\pi}{N} + 8\varepsilon(a - 2r_k^2)\cos\frac{2k\pi}{N}\right)\sin^2\frac{j\pi}{N}. \tag{32}$$

Again using inequality (28), we get

$$\beta_{j,min} = \beta_1 \geq 0, \tag{33}$$

and then

$$a \geq \varepsilon \frac{4\sin^2(\frac{k\pi}{N})(1 + 2\cos(\frac{2k\pi}{N})) - 2\sin^2(\frac{\pi}{N})}{\cos(\frac{2k\pi}{N})}. \tag{34}$$

Mathematical analysis shows that this β condition is more restricted than the α condition (or, equivalently, the existence condition) except in three extreme cases: One is $k = 0$, the second is $k = \frac{N}{2}$ for even N, and the third is $k = \frac{N-1}{2}$ for odd N. For the first two cases, the α condition is more restricted than the β condition, and for the last case, the α condition is equivalent to the β condition. This is not surprising; as both $k = 0$ and $k = [\frac{N}{2}]$ modes are born due to the instability of the homogeneous steady state by Hopf bifurcations (see the analysis in section 3 and Figure 1(a)) and all other k modes are generated by saddle-node bifurcations, from the knowledge of bifurcation theory we know that their stability should be determined by the α and β conditions, respectively.

We explicitly show the stability distribution of all splay states for different k's in the (a, ε) phase diagram in Figure 3(a), according to the β condition in (34), except for the vertical curve for the $k = 0$ mode ($a = 0$ and $\varepsilon > 0$), whose stability is controlled by the α condition.

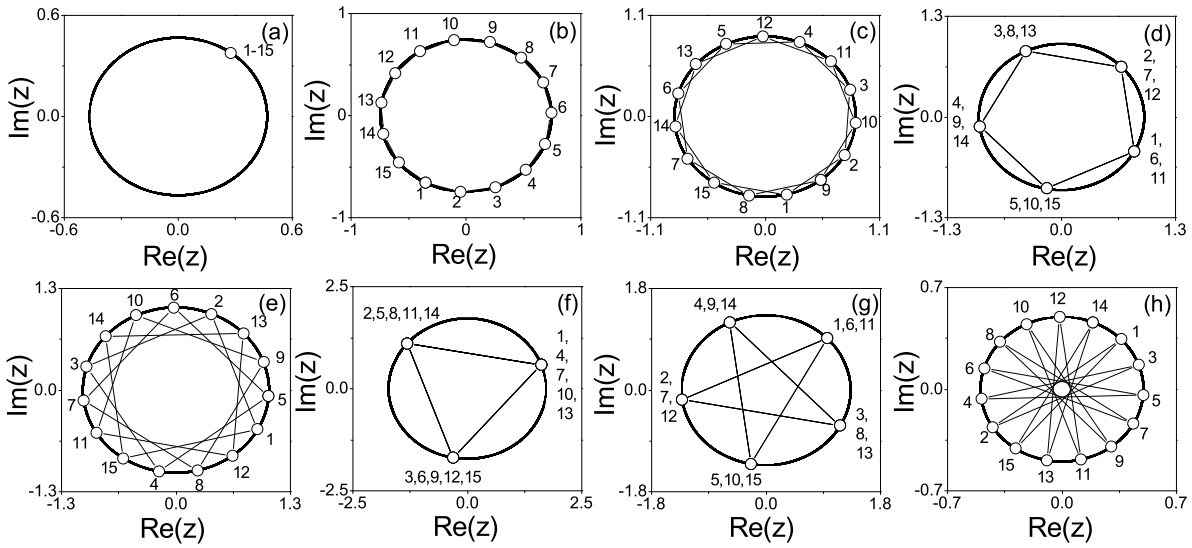

Figure 4. (a)–(h) *The structures of the stable splay states of modes from* $k = 0$ *to* 7 *for* $\theta_0 = 1.35$, $\theta_1 = 0.82$, $\theta_2 = 0.3$, $\theta_3 = 0.08$, $\theta_4 = 6.23$, $\theta_5 = 5.4$, $\theta_6 = 3.9$, *and* $\theta_7 = 3.45$ *on the unit circle (triangles on the dashed circle in Figure* 3(a)*), respectively.* $d = 1$.

From $k = 0$ to $k = 7$ modes, their critical curves should be separated for different k's, and in particular their stable regimes should be located within the range of polar angles: $0 < \theta_0 < \frac{\pi}{2}$, $0 < \theta_1 < 1.16$, $0 < \theta_2 < 0.43$, $0 < \theta_3 < 0.14$, $6.22 < \theta_4 < 2\pi$, $4.54 < \theta_5 < 2\pi$, $3.48 < \theta_6 < 2\pi$, and $3.39 < \theta_7 < 2\pi$, respectively. Numerical results for the stable regimes of each k in Figure 3(b) and their corresponding stable attractors in the phase space ($\theta_0 = 1.35$, $\theta_1 = 0.82$, $\theta_2 = 0.3$, $\theta_3 = 0.08$, $\theta_4 = 6.23$, $\theta_5 = 5.4$, $\theta_6 = 3.9$, and $\theta_7 = 3.45$ on the unit circle and within their corresponding stable parameter regimes) in Figure 4 well confirm our prediction.

The blank region in Figure 3(b) just denotes the stable region of the homogeneous steady state. We also find that in the (a, ε) space the critical curves of all modes are distributed regularly in a clockwise direction, and the modes $0 \le k < \frac{N}{4}$ stay at the upper part of the (a, ε) space ($\varepsilon > 0$) and the modes $\frac{N}{4} < k \le \frac{N}{2}$ stay at the lower part ($\varepsilon < 0$). All these findings can be easily proved by using manipulation of some algebra on the β condition. In addition, an interesting byproduct is the occurrence of multistability of splay states. Clearly the size of the stable region of mode 0 is much larger than that of modes 1, 2, and 3, and the size of the stable region of mode 7 is much larger than that of modes 4, 5, and 6; see Figure 3(a). The impact of multistability becomes more remarkable at the region near the line $\varepsilon = 0$ and $a > 0$; for a slightly positive ε (phase-attractive coupling), all modes $0 \le k < \frac{N}{4}$ are stable, and, oppositely, for a slightly negative ε (phase-repulsive coupling), all modes $\frac{N}{4} < k \le \frac{N}{2}$ are stable.

4.3. Global coupling. Considering the case for global coupling ($d = \frac{N-1}{2}$ for odd N), we have

$$r_k = \sqrt{a - N\varepsilon}, \tag{35}$$

which is independent of k,

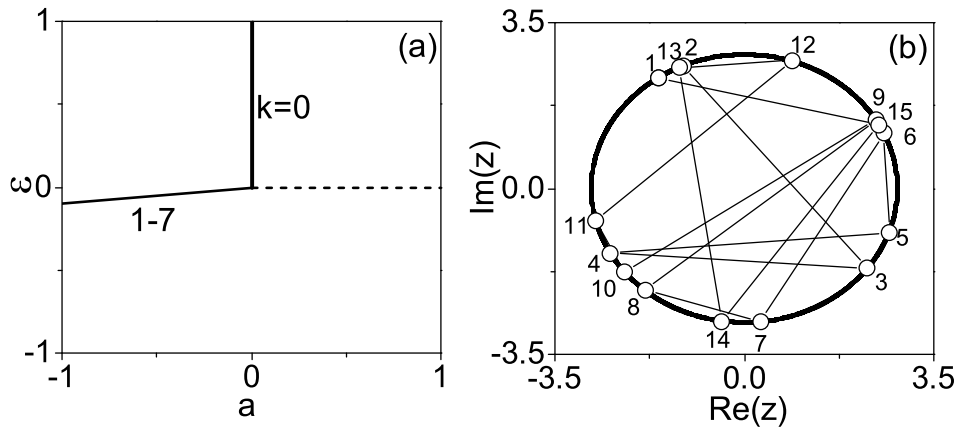

Figure 5. *The study of the global coupling* ($d = \frac{N-1}{2} = 7$). (a) *The stable regimes of the homogeneous steady state and the splay states for all different modes. The stable regime of the homogeneous steady state is exactly located at the first quadrant; this feature is unchanged for different d's. Oppositely, the stable regimes of the splay states for all nonzero modes are surrounded by the same sloped critical curve and the horizontal (dashed) curve.* (b) *The periodic orbit and snapshot of oscillators from random initial conditions. The parameters are* $a = 0.5$ *and* $\varepsilon = -0.5$.

$$\sigma_{k+j} = -N, \tag{36}$$

and

$$\sigma_{k-j} = \begin{cases} -N & \text{if } j \neq k, \\ 0 & \text{if } j = k. \end{cases} \tag{37}$$

Therefore, we have

$$\begin{cases} \alpha_j = -2r_k^2, \quad \beta_j = 0 & \text{if } j = 0, 1, \ldots, [\frac{N}{2}] \text{ and } j \neq k, \\ \alpha_j = -2r_k^2 + N\varepsilon, \quad \beta_j = -r_k^2 N\varepsilon & \text{if } j = k. \end{cases} \tag{38}$$

After considering the existence condition (inequality (5)) and the α and β conditions (inequalities (25) and (26)), we can easily obtain that all these modes for $k \neq 0$ are degenerated (with the same stability), and their stability is determined by

$$a > N\varepsilon, \ \varepsilon < 0. \tag{39}$$

We also know that their stability is neutral (with $N - 2$ zero eigenvalues), and they can exist in a very broad parameter space. In sharp contrast to this, for the local coupling discussed in the previous section, the neutral stability of splay states can occur only at the position of the corresponding critical curves of each mode. We illustrate their stable regimes in Figure 5(a), which also includes the stable regime of the in-phase state. The attractor and snapshot with randomly distributed structure (general splay state) from random initial conditions are shown in Figure 5(b), which is qualitatively similar to the plot in Figure 2(f). This time the parameter set $a = 0.5$ and $\varepsilon = -0.5$, which is deep into the stable regime, is chosen. The stability of the general splay state is the same as that of the equally distributed splay state; for more detailed analysis, see Appendix B.

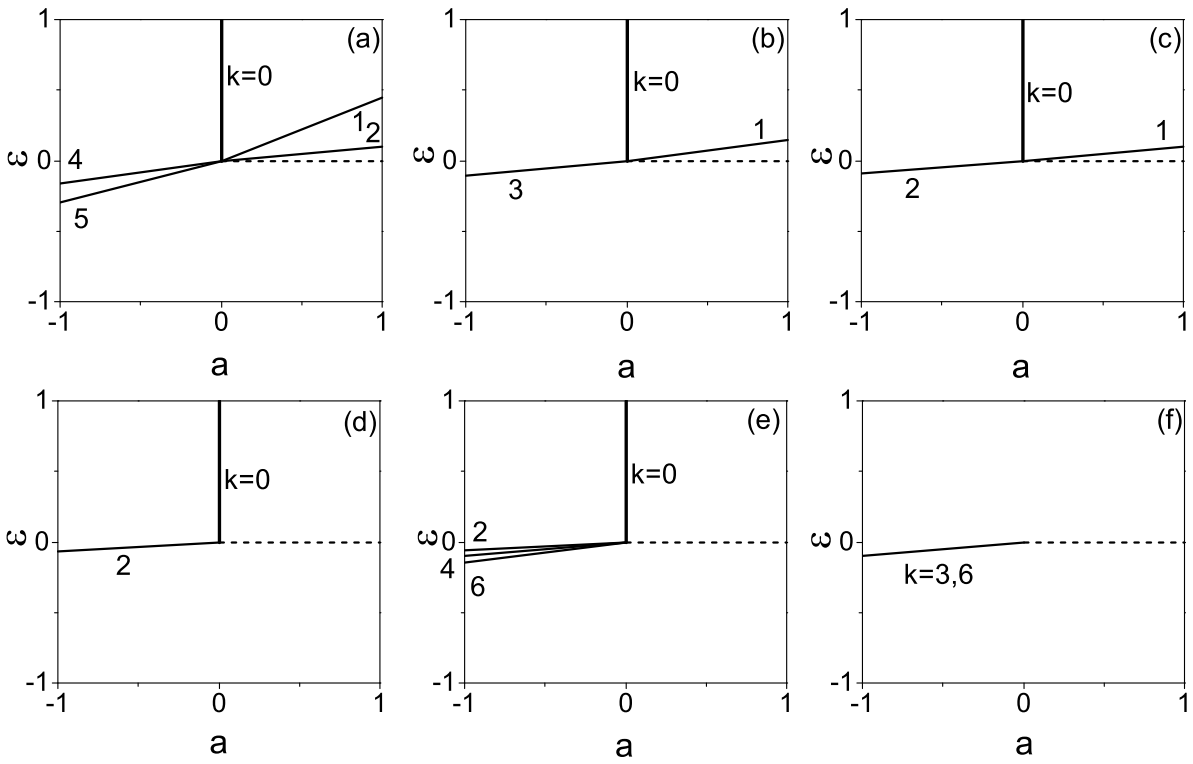

Figure 6. *The study of the intermediate-range coupling for different d's.* (a)–(e) *The stable regimes of splay states for d from $d = 2$ to 6, respectively.* (f) *The neutrally stable regimes of splay states of the $k = 3$ and 6 modes. $d = 4$.*

4.4. Intermediate-range coupling. For intermediate-range coupling, we have to first consider the existence condition (5) and then both the α (inequality (25)) and β (inequality (26)) conditions. There is no easy way to obtain the explicit expression for the stability of each mode, but clearly the problem has already been much simplified and the number of zero eigenvalues from the linear stability analysis can be easily calculated from simulations. We plot the stable regimes of splay states from $d = 2$ to 6 with the increase of coupling range in Figures 6(a)–6(e), respectively. Again, all stable regimes are surrounded by the critical curve and the horizontal curve ($\varepsilon = 0$ and $a > 0$, the dashed lines in the figures). Interestingly, we find that the sequence of these modes may begin to get disordered; e.g., the critical curve of mode 4 is above that of mode 5 for $d = 2$ in Figure 6(a), and the order of the critical curves of modes 2, 4, and 6 get completely disordered for $d = 6$ in Figure 6(e). We also find that some modes may even have no stable regimes; e.g., the stable regime of mode 3 disappears for $d = 2$, 5, and 6, and that of mode 7 disappears completely for any d from $d = 2$ to 6; see Figure 6 for details. This behavior is similar to the prohibited state in quantum mechanics. All these are clearly distinct from the cases of both local coupling and global coupling. However, similar to global coupling, the neutral stability may begin to appear for certain k and d; e.g., see Figure 6(f) for $k = 3$ and 6 and $d = 4$. Their orbits are exhibited in Figures 7(a) and 7(b) for $k = 3$ and 6, respectively. The parameters are $a = 0.5$ and $\varepsilon = -0.5$. Further study finds that the systems may show an unusual cluster behavior with several copies of general splay

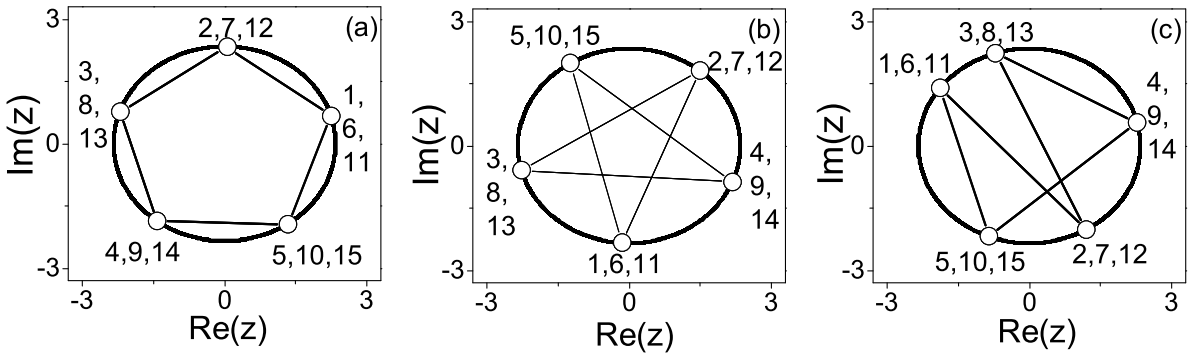

Figure 7. *The orbits and snapshots of the coupled systems for $d = 4$, $a = 0.5$, and $\varepsilon = -0.5$.* (a)–(b) *The neutrally stable splay states for the $k = 3$ and 6 modes, respectively.* (c) *The unusual splay state in systems with intermediate-range coupling, showing several copies of the general splay state of small-size systems.*

state of smaller-size systems, as shown in Figure 7(c) with the same parameters as in Figures 7(a) and 7(b). Note that this behavior is very generic.

5. Discussion. In summary, we have systematically studied the existence and stability conditions of the homogeneous steady state and splay states for different cases from local to global coupling via intermediate-range coupling. For the two extreme cases (local and global couplings), explicit results are analytically obtained. These analyses allow us to obtain more detailed knowledge about the stability (and/or instability), structure, and organization of splay states and their relations with the homogeneous steady state and the in-phase state. Similar phenomena have been found in other systems, such as the coupled periodic Rossler systems and the coupled Van der Pol oscillators. From these observations, we know that the range of coupling plays a significant role in the organization of various dynamical behaviors. For these different connection configurations, on the one hand, they may share some common features, such as the upper-left corner stable regime of the homogeneous steady state in the (a, ε) parameter space, the uniform upper-right corner stable regime of the in-phase state, and the radiating structure of critical curves all emanating from the origin (this feature can be easily analyzed from the existence and stability conditions). On the other hand, the different range of coupling brings some unique characteristics indeed. For local coupling, the critical curves appear to be distributed orderly and regularly scattered. As opposed to this, for global coupling, all the critical curves ($k \neq 0$) are degenerated and adhered together. Differently, as a bridge of the local and global couplings, the stability of splay states with an intermediate range of coupling shows its own properties. The critical curves begin to be distributed disorderly and some of them may even disappear completely. Some behaviors such as the neutral stability and general splay state, which were generally reported on the systems with global coupling, may begin to appear in a novel manner. As the studies of the model of coupled Landau–Stuart oscillators are important in nonlinear science, we hope that all these findings can help us understand splay states and relevant dynamical behaviors in a unified way. They are also expected to have potential applications (such as in Josephson-junction arrays, electronic circuits, coupled laser systems, and biological systems as well) and to be observable in experiments.

Appendix A. Some useful matrices and their relations. Some useful matrices are as follows.

(1) The circular matrix B is

$$B = \mathrm{circ}(b_1, b_2, \ldots, b_N), \tag{40}$$

where the matrix elements $b_1 = -2d$, $b_{j+1} = b_{N-j+1} = 1$ for $j = 1, \ldots, d$ and $b_j = 0$ for other j.

(2) The Fourier matrix P is

$$P = (p_{k,m})_{k,m=0,\ldots,N-1}, \tag{41}$$

where $p_{k,m} = e^{i\frac{km2\pi}{N}}$.

(3) The diagonal matrix P_k is

$$P_k = \mathrm{diag}(p_{0,k}, \ldots, p_{N-1,k}), \tag{42}$$

where $p_{j,k} = e^{i\frac{jk2\pi}{N}}$, $j = 0, \ldots, N-1$.

(4) The mirror symmetry matrix S is

$$S = \begin{pmatrix} 1 & 0 & \ldots & 0 \\ 0 & 0 & & 1 \\ \vdots & & \ddots & \\ 0 & 1 & & 0 \end{pmatrix}. \tag{43}$$

Some relations between them are

$$P^{-1}BP = \Lambda_0 = \mathrm{diag}(\sigma_0, \ldots, \sigma_{N-1}), \tag{44}$$

where $\sigma_k = -4\sum_{m=1}^{d} \sin^2(\frac{mk\pi}{N})$, $k = 0, \ldots, N-1$,

$$(P_kP)^{-1}B(P_kP) = \Lambda_k = \mathrm{diag}(\sigma_k, \ldots, \sigma_{k+N-1}), \tag{45}$$

and

$$(P_kP)^{-1}P_k^2\overline{(P_kP)} = P^{-1}\overline{P} = S, \tag{46}$$

where A^{-1} denotes the inverse matrix of A and $\overline{A}$ denotes the conjugate matrix of A (A is an arbitrary matrix).

Appendix B. The stability of the general splay state. For the globally coupled Landau–Stuart oscillators

$$\dot{z_j} = (a + i\omega - |z_j|^2)z_j + \varepsilon\sum_{s=1}^{N}(z_s - z_j), \quad j = 1, \ldots, N, \tag{47}$$

the general splay state solution can be expressed as

$$z_j = re^{i\theta_j} = \sqrt{a - N\varepsilon}e^{i(\omega t+\varphi_j)}, \quad j = 1, \dots, N, \quad \text{with} \quad \sum_{j=1}^{N} e^{i\varphi_j} = 0. \tag{48}$$

To determine its stability, we introduce the small perturbation variables ξ_j, defined as

$$z_j = \sqrt{a - N\varepsilon}e^{i(\omega t+\varphi_j)}(1 + \xi_j), \quad j = 1, \dots, N. \tag{49}$$

The linearized equations around the general splay state can be obtained as

$$\dot{\xi}_j = -r^2\xi_j - r^2\overline{\xi_j} + \varepsilon \sum_{s=1}^{N} e^{i(\varphi_s-\varphi_j)}\xi_s, \quad j = 1, \dots, N. \tag{50}$$

Let us introduce two macrovariables

$$E = \frac{1}{N}\sum_{s=1}^{N} e^{i\varphi_s}\xi_s \quad \text{and} \quad F = \frac{1}{N}\sum_{s=1}^{N} e^{i\varphi_s}\overline{\xi}_s. \tag{51}$$

A subspace in the whole perturbation space $\{\xi_s\}$ determined by $E = F = 0$ constitutes an invariant subspace, in which the perturbations evolve as

$$\dot{\xi}_j = -r^2\xi_j - r^2\overline{\xi_j} \tag{52}$$

and

$$\dot{\overline{\xi}}_j = -r^2\overline{\xi_j} - r^2\xi_j. \tag{53}$$

From (52) and (53), we obtain the eigenvalues $\lambda = 0$ and $-2r^2 < 0$, both of which are $(N-2)$-fold degenerate. All these eigenvalues are stable or marginally stable. The perturbations transversal to the invariant subspace obey the equations

$$\dot{E} = (-r^2 + N\varepsilon)E - r^2F, \tag{54}$$

$$\dot{\overline{E}} = (-r^2 + N\varepsilon)\overline{E} - r^2\overline{F}, \tag{55}$$

$$\dot{F} = -r^2E - r^2F + N\varepsilon\Delta\overline{E}, \tag{56}$$

$$\dot{\overline{F}} = -r^2\overline{E} - r^2\overline{F} + N\varepsilon\overline{\Delta}E, \tag{57}$$

where $\Delta = \frac{1}{N}\sum_{j=1}^{N} e^{2i\varphi_j}$, $0 \le |\Delta| \le 1$. The associated eigenvalues determined by (54)–(57) can be obtained from

$$\lambda^2 - (-2r^2 + N\varepsilon)\lambda - r^2N\varepsilon(1 \pm |\Delta|) = 0. \tag{58}$$

It is easy to see that all four eigenvalues of (58) are stable if and only if $\varepsilon < 0$; thus the stability of the general splay state is determined by

$$a > N\varepsilon, \ \varepsilon < 0, \tag{59}$$

which is the same as the condition for the stability of the equally distributed splay states in globally coupled Landau–Stuart oscillators (see (39)).

Acknowledgment. The authors would like to thank the anonymous referees for their helpful comments which have helped to improve the paper.

REFERENCES

[1] A. T. Winfree, *The Geometry of Biological Time*, Springer-Verlag, New York, 1980.
[2] Y. Kuramoto, *Chemical Oscillations, Waves, and Turbulence*, Springer-Verlag, Berlin, 1984.
[3] A. Pikovsky, M. Rosenblum, and J. Kurths, *Synchronization: A Universal Concept in Nonlinear Dynamics*, Cambridge University Press, Cambridge, UK, 2001.
[4] J. D. Murray, *Mathematical Biology*, Springer-Verlag, Berlin, 2003.
[5] P. Hadley and M. R. Beasley, *Dynamical states and stability of linear arrays of Josephson-junctions*, Appl. Phys. Lett., 50 (1987), pp. 621–623.
[6] K. Wiesenfeld and P. Hadley, *Attractor crowding in oscillator arrays*, Phys. Rev. Lett., 62 (1989), pp. 1335–1338.
[7] K. Y. Tsang and K. Wiesenfeld, *Attractor crowding in Josephson-junction arrays*, Appl. Phys. Lett., 56 (1990), pp. 495–496.
[8] K. Y. Tsang and I. B. Schwartz, *Interhyperhedral diffusion in Josephson-junction arrays*, Phys. Rev. Lett., 68 (1992), pp. 2265–2268.
[9] S. Nichols and K. Wiesenfeld, *Ubiquitous neutral stability of splay-phase states*, Phys. Rev. A, 45 (1992), pp. 8430–8435.
[10] S. H. Strogatz and R. E. Mirollo, *Splay states in globally coupled Josephson arrays: Analytical prediction of Floquet multipliers*, Phys. Rev. E, 47 (1993), pp. 220–227.
[11] S. Nichols and K. Wiesenfeld, *Non-neutral dynamics of splay states in Josephson-junction arrays*, Phys. Rev. E, 50 (1994), pp. 205–212.
[12] D. G. Aronson, M. Golubitsky, and J. Mallet-Paret, *Ponies on a merry-go-round in large arrays of Josephson junctions*, Nonlinearity, 4 (1991), pp. 903–910.
[13] P. Ashwin, G. P. King, and J. W. Swift, *Three identical oscillators with symmetric coupling*, Nonlinearity, 3 (1990), pp. 585–601.
[14] P. L. Várkonyi and P. Holmes, *On synchronization and traveling waves in chains of relaxation oscillators with an application to Lamprey CPG*, SIAM J. Appl. Dyn. Syst., 7 (2008), pp. 766–794.
[15] K. Wiesenfeld, C. Bracikowshi, G. E. James, and R. Roy, *Observation of antiphase states in a multimode laser*, Phys. Rev. Lett., 65 (1990), pp. 1749–1752.
[16] G. E. James and E. M. Harrell, *Intermittency and chaos in intracavity doubled lasers* II, Phys. Rev. A, 41 (1990), pp. 2778–2790.
[17] K. Otsuka, *Winner-takes-all dynamics and antiphase states in modulated multimode lasers*, Phys. Rev. Lett., 67 (1991), pp. 1090–1093.
[18] M. Silber, L. Fabiny, and K. Wiesenfeld, *Stability results for in-phase and splay-phase states of solid-state laser arrays*, J. Opt. Soc. Amer. B Opt. Phys., 10 (1993), pp. 1121–1129.
[19] W. J. Rappel, *Dynamics of a globally coupled laser model*, Phys. Rev. E, 49 (1994), pp. 2750–2755.
[20] J. W. Swift, S. H. Strogatz, and K. Wiesenfeld, *Averaging of globally coupled oscillators*, Phys. D, 55 (1992), pp. 239–250.
[21] T. W. Carr and I. B. Schwartz, *Symmetry-breaking control of splay-phase states in globally coupled oscillators*, Phys. Lett. A, 227 (1997), pp. 41–46.
[22] A. Takamatsu, R. Tanaka, H. Yamada, T. Nakagaki, T. Fujii, and I. Endo, *Spatiotemporal symmetry in rings of coupled biological oscillators of Physarum plasmodial slime mold*, Phys. Rev. Lett., 87 (2001), 078102.
[23] A. Takamatsu, R. Tanaka, and T. Fujii, *Hidden symmetry in chains of biological coupled oscillators*, Phys. Rev. Lett., 92 (2004), 228102.
[24] Y. Morita, *A periodic wave and its stability to a circular chain of weakly coupled oscillators*, SIAM J. Math. Anal., 18 (1987), pp. 1681–1698.
[25] C. R. Laing, *Rotating waves in rings of coupled oscillators*, Dyn. Syst., 13 (1998), pp. 305–318.
[26] G. Hu, F. G. Xie, Z. L. Qu, and P. L. Shi, *Antiphase states in coupled oscillator system*, Commun. Theor. Phys. (Beijing), 33 (1999), pp. 99–106.

[27] G. Hu, Y. Zhang, H. A. Cerdeira, and S. G. Chen, *From low-dimensional synchronous chaos to high-dimensional desynchronous spatiotemporal chaos in coupled systems*, Phys. Rev. Lett., 85 (2000), pp. 3377–3380.
[28] H. L. Yang, *Phase synchronization of diffusively coupled Rossler oscillators with funnel attractors*, Phys. Rev. E, 64 (2001), 026206.
[29] M. Zhan, G. Hu, Y. Zhang, and D. H. He, *Generalized splay state in coupled chaotic oscillators induced by weak mutual resonant interactions*, Phys. Rev. Lett., 86 (2001), pp. 1510–1513.
[30] D. H. He, G. Hu, M. Zhan, and H. P. Lu, *Periodic states with functional phase relation in weakly coupled chaotic Hindmarsh-Rose neurons*, Phys. D, 156 (2001), pp. 314–324.
[31] M. Zhan and R. Kapral, *Model for line defects in complex-oscillatory spiral waves*, Phys. Rev. E, 72 (2005), 046221.
[32] M. Zhan and R. Kapral, *Destruction of spiral waves in chaotic media*, Phys. Rev. E, 73 (2006), 026224.
[33] D. G. Aronson, G. B. Ermentrout, and N. Kopell, *Amplitude response of coupled oscillators*, Phys. D, 41 (1990), pp. 403–449.
[34] D. V. R. Reddy, A. Sen, and G. L. Johnston, *Time delay induced death in coupled limit cycle oscillators*, Phys. Rev. Lett., 80 (1998), pp. 5109–5112.
[35] J. Z. Yang, *Transitions to amplitude death in a regular array of nonlinear oscillators*, Phys. Rev. E, 76 (2007), 016204.
[36] A. Palacios, A. Carretero-Gonzalez, P. Longhini, and N. Renz, *Multifrequency synthesis using two coupled nonlinear oscillator arrays*, Phys. Rev. E, 72 (2005), 026211.
[37] A. S. Landsman and I. B. Schwartz, *Predictions of ultraharmonic oscillations in coupled arrays of limit cycle oscillators*, Phys. Rev. E, 74 (2006), 036204.
[38] K. Ito and Y. Nishiur, *Intermittent switching for three repulsively coupled oscillators*, Phys. Rev. E, 77 (2008), 036224.
[39] H. Daido and K. Nakanishi, *Diffusion-induced inhomogeneity in globally coupled oscillators: Swing-by mechanism*, Phys. Rev. Lett., 96 (2006), 054101.
[40] H. Daido and K. Nakanishi, *Aging transition and universal scaling in oscillator networks*, Phys. Rev. Lett., 93 (2004), 104101.
[41] H. Daido and K. Nakanishi, *Aging and clustering in globally coupled oscillators*, Phys. Rev. E, 75 (2007), 056206.
[42] H. Daido, *Aging transition and disorder-induced coherence in locally coupled oscillators*, Europhys. Lett., 84 (2008), 10002.
[43] S. Yanchuk and M. Wolfrum, *Destabilization patterns in chains of coupled oscillators*, Phys. Rev. E, 77 (2008), 026212.